AGU ADVANCING EARTH AND SPACE SCIENCE

Geophysical Research Letters

RESEARCH LETTER

10.1029/2022GL100505

Causes of Missing Snowmelt Following Drought

Dana A. Lapides[1,2], W. Jesse Hahm[2], Daniella M. Rempe[3], John Whiting[1], and David N. Dralle[1]

[1]Pacific Southwest Research Station, United States Forest Service, Davis, CA, USA, [2]Department of Geography, Simon Fraser University, Burnaby, BC, Canada, [3]University of Texas at Austin, Austin, TX, USA

Key Points:

- At 15 watersheds in the Sierra Nevada, the root-zone storage deficit explains anomalously low streamflow from snowpack following drought
- Median error in 2021 predictions is reduced from 60% to 20% by including the deficit in the forecasting model
- Future drought-related perturbations to runoff could be assessed using root-zone storage deficits inferred from distributed hydrologic data

Supporting Information:

Supporting Information may be found in the online version of this article.

Correspondence to:

D. A. Lapides,
dlapides@sfu.ca

Citation:

Lapides, D. A., Hahm, W. J., Rempe, D. M., Whiting, J., & Dralle, D. N. (2022). Causes of missing snowmelt following drought. *Geophysical Research Letters*, *49*, e2022GL100505. https://doi.org/10.1029/2022GL100505

Received 20 JUL 2022
Accepted 22 SEP 2022

Abstract Water management in snowy mountainous regions hinges on forecasting snowmelt runoff. However, droughts are altering snowpack-runoff relationships with ongoing debate about the driving mechanisms. For example, in 2021 in California, less than half of predicted streamflow arrived. Mechanisms proposed for this "missing" streamflow included changes in evapotranspiration (*ET*), rainfall, and subsurface moisture conditions. Here, we demonstrate that *ET* in drought years generates dry subsurface conditions that reduce runoff in subsequent years. A model including this legacy of depleted moisture storage reduced median error in 2021 forecasts from 60% to 20% at 15 minimally disturbed basins and from 18% to 2% at 6 water supply basins in the Sierra Nevada (basins range in area from 5 to 23,051 km^2 and mean annual precipitation from 814 to 1,549 mm). Our findings indicate that the relationship between snowpack and runoff will evolve as plant ecosystems respond to climate change and alter subsurface water storage dynamics.

Plain Language Summary Essential water supply from snowpack may become more difficult to predict as the climate changes. Following a recent drought in California, the traditionally used model for snowmelt runoff failed. Here, we present a model that accounts for this model failure by incorporating the role of root-zone storage dynamics in the production of snowmelt runoff. Through transpiration, montane forests generate water storage deficits in the soils and weathered bedrock that comprise the root-zone. These deficits must be replenished by rain and snowmelt before significant runoff generation can occur. Overprediction of 2021 post-drought runoff in California can be primarily attributed to unprecedentedly large root-zone storage deficits.

1. Introduction

Mountain snowpack is an essential water reservoir for 1.9 billion people globally (Immerzeel et al., 2020). However, the accessibility of this water depends on how snowmelt runoff is generated. Historically, managers have relied on statistical relationships between snowpack and subsequent runoff for forecasting (DeWalle & Rango, 2008), but changes in climate can alter these relationships. Recently, in 2021 following a severe drought in California, streamflow forecasts by historically reliable multiple linear regression snowpack-runoff relationships (California Department of Water Resources, 2021) far exceeded actual streamflow (see e.g., Figures 1a and 1b and site-specific versions of this figure in the Data Supplement in Lapides et al. (2021, the github/zenodo archive)). This led scientists and the public alike (Canon, 2021; Rogers, 2021) to wonder—where did the missing snowmelt go?

This change from historical conditions is a signal of "nonstationarity" in streamflow generation (Bayazit, 2015), falling in line with predictions that dwindling snowpack would make droughts less predictable (Livneh & Badger, 2020; Vano, 2020). Previous work has proposed that such shifts in streamflow generation from a given water input (snowpack) arise from differences in evapotranspiration (*ET*) due to changes in evaporative demand (Avanzi et al., 2020; Hamlet et al., 2007; Hoerling & Eischeid, 2007), snowmelt rate (Barnhart et al., 2016), vegetation community (Boon, 2009; Knight et al., 1991; Pugh & Small, 2012), and/or changes to the energy balance due to changes in albedo with less snowpack (Livneh & Badger, 2020; Milly & Dunne, 2020; Vano, 2020). This effect may be particularly strong during multi-year droughts when *ET* can be a larger fraction of the annual water budget than usual (Massari et al., 2022). Antecedent moisture conditions have also been proposed to alter the relationship between water inputs and resulting streamflow (Avanzi et al., 2020; Hawkins & Ellis, 2010; Penna et al., 2011, 2015), including the role of rainfall inputs during the winter season and subsurface moisture conditions at the start of the winter season. Both of these factors can be tied to a form of runoff generation in which significant runoff occurs only after infiltrating water replenishes subsurface storage (McDonnell et al., 2021; Sayama et al., 2011). After the subsurface dries—typically through withdrawal of root-zone moisture by *ET*

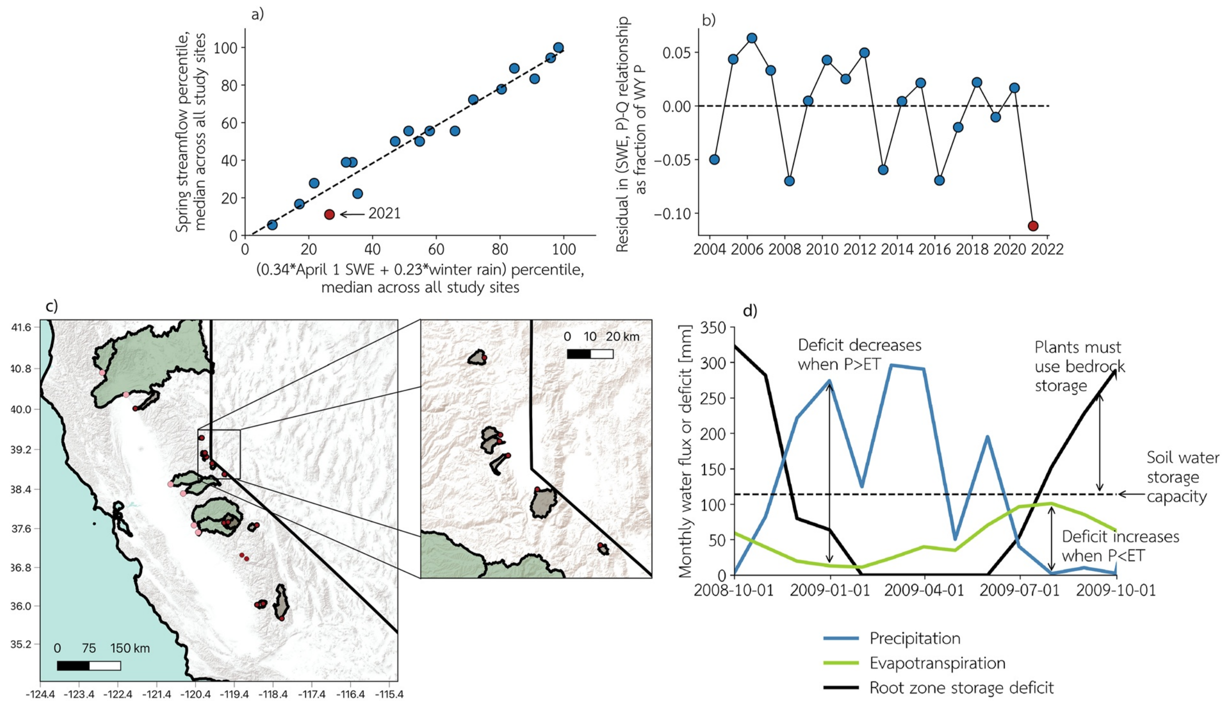

Figure 1. (a) Relationship between regression model for streamflow based on April 1 snow water equivalent (SWE) and winter rain and measured spring (April-July) streamflow summarized at 15 minimally disturbed sites for each year within the study period (2004–2021). This model is of a similar form to the one used by the California Department of Water Resources for streamflow forecasting. Points above the dashed line are years when the linear model underpredicts streamflow, and below the dashed line are years when the model overpredicts streamflow. SWE data is from Snow Data Assimilation System (National Operational Hydrologic Remote Sensing Center, 2000). Mean absolute error from leave-one-out cross-validation is 18 percentile points. (b) Median residual in the SWE-streamflow relationship among minimally disturbed sites as a fraction of April 1 SWE. Outlier holds for all water supply basins and all but four minimally disturbed sites (see Data Supplement in Lapides et al. (2021, the github/zenodo archive)). (c) Map of study watersheds in the Sierra Nevada. Red dots mark gage locations for minimally disturbed sites shaded in gray, and pink dots for water supply basins shaded in green. (d) Explanatory plot for root-zone storage deficit. At the beginning of the wet season, the deficit decreases to 0 and remains there until evapotranspiration exceeds P in the dry season. Deficit grows until the beginning of the next wet season. Deficits larger than soil water storage capacity indicate plant use of water stored in weathered bedrock.

as shown in Figure 1d (Arkley, 1981; Bales et al., 2011; Goulden & Bales, 2019; Hahm et al., 2020; Jones & Graham, 1993; Klos et al., 2018; Lewis & Burgy, 1964; M. Anderson et al., 1995; McCormick et al., 2021; Miller et al., 2010; Rempe & Dietrich, 2018; Rose et al., 2003; Sayama et al., 2011)—infiltrating water goes first to replenishing this moisture deficit and then toward generating streamflow (McDonnell et al., 2021; Sayama et al., 2011). Less water input prior to snowmelt (i.e., winter rainfall) or more *ET* during or prior to snowmelt (i.e., winter and spring *ET*) can limit how quickly the storage deficit is replenished—the precondition for significant streamflow generation. In this way, subsurface moisture conditions interact with above-ground factors to mediate runoff generation from snowpack.

Subsurface moisture deficits describe conditions in soils as well as the underlying weathered bedrock, which can account for a large portion of root-zone water storage (Bales et al., 2011; Ichii et al., 2009; K. J. K. J. Fowler et al., 2021; McCormick et al., 2021). Soil moisture has been identified as a skillful predictor of streamflow (e.g., Harpold et al., 2017; Koster et al., 2010), and prior studies have generally estimated soil moisture from soils data sets (Li et al., 2013), models that rely on soil data sets for parameterization (Mahanama et al., 2012), or shallow and sparse in situ observations of soil moisture (Harpold et al., 2017). While helpful, soil-based predictors may not capture deeper plant-mediated water storage dynamics that occur in underlying bedrock. Although there have been advances in large-scale observation of shallow soil moisture conditions (Entekhabi et al., 2010), deeper storage is less easy to monitor (Rempe & Dietrich, 2018) but still important for the water balance (McCormick et al., 2021). Further, while storage changes recorded by the Gravity Recovery and Climate Experiment (GRACE) have been shown to be a strong predictor of subsequent streamflow (Sproles et al., 2015), GRACE data are not finely resolved and include water storage effects (e.g., deep groundwater) that may not be relevant to the root-zone. Modeled subsurface water storage is, due to limited availability of deep water storage

10.1029/2022GL100505

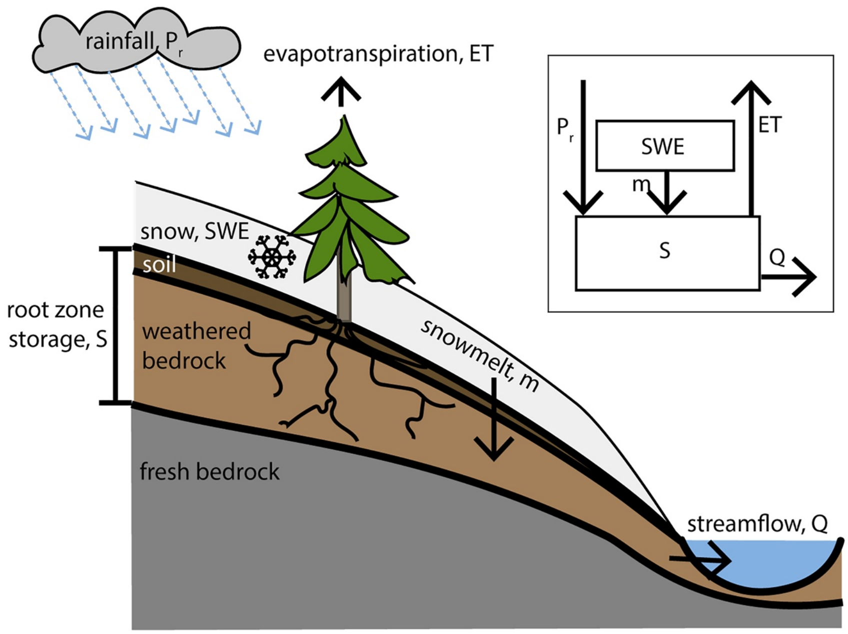

Figure 2. Conceptual hillslope diagram of mountain hydrology. Thin soils cover a deep, weathered bedrock zone that plants may access throughout the dry season. Snow accumulates during the winter and subsequently melts into the subsurface, while rain directly replenishes the subsurface. Evapotranspiration reduces water in storage, and streamflow is generated once a subsurface storage deficit is replenished. The inset diagram shows the two modeled water reservoirs (snow and root-zone storage) and fluxes (rainfall, snowmelt, evapotranspiration, and streamflow).

information, contingent on parameterization from available soil textural databases, which cannot account for storage dynamics in underlying bedrock (K. Fowler et al., 2020). The Climatic Water Deficit (CWD) is an alternative method of estimating water stress or water availability that has been shown to be a strong indicator of drought (e.g., Garcia-Barreda & Camarero, 2020; Paltineanu et al., 2009), but CWD is a heuristic drought stress indicator rather than a physical state variable.

An alternative approach for estimating storage deficits is to track the balance between fluxes entering and exiting the root-zone, which quantifies root zone water storage. Spatially distributed, near real-time plant-driven water storage dynamics throughout both soil and bedrock can thus be quantified from precipitation and *ET* time-series (Dralle et al., 2021; Roche et al., 2020; Wang-Erlandsson et al., 2016). These estimates of storage deficits provide a full accounting of plant-accessible water stored throughout soils and deeper weathered bedrock using a data-driven method with very few underlying assumptions. Considering storage deficits in runoff prediction (Grindley, 1960) or as a harbinger of drought (Geruo et al., 2017; Thomas et al., 2014) is not new, but the widespread availability of distributed and increasingly reliable *ET* (Zhang et al., 2019), precipitation (Wang-Erlandsson et al., 2016), snow cover (as used by Dralle et al., 2021), and snow water equivalent (SWE) (Wrzesien et al., 2017) data sets now make it possible to monitor deficits in mountainous regions at large scales.

In this study, we introduce a mass-balance model for snowmelt driven runoff in a Mediterranean environment (wet winter, dry growing season) that explicitly incorporates the root-zone water storage deficit (encompassing both the soil and underlying bedrock) estimated from distributed data products to explore the following hypothesized explanations for snowmelt runoff reduction (see Figure 2 for a schematic):

1. Less rainfall fell than normal during the spring;
2. Snowmelt rate was slower than normal;
3. Evaporative demand was higher than normal during the winter;
4. Evaporative demand was higher than normal during the spring; and
5. The root-zone water storage deficit at the start of the wet season was larger than normal.

We validate our mass balance model against observed spring streamflow at 15 minimally disturbed sites in the Sierra Nevada and then develop a multiple linear regression model to quantify which drivers have the largest impact on snowmelt runoff. Based on results from the multiple linear regression analysis, we quantify improvement in snowmelt runoff forecasts in 2021 at 15 minimally disturbed watersheds as well as 6 watersheds important for California's water supply. While we specifically explore the fate of the "missing" 2021 snowmelt runoff in California, our goal is to understand how subsurface water storage dynamics—in combination with other previously studied mechanisms—inform forecasting of snowmelt runoff in general.

2. Methods

2.1. Mass-Balance Snowmelt Runoff Model

Here we expand upon a stochastic hydrological model (Hahm et al., 2019) that incorporates storage as a simple 1-d bucket to describe annual runoff dynamics and plant water availability in Mediterranean catchments. In the original model, precipitation P [L] contributes water to storage during the wet season, and ET [L] removes water from storage primarily during the dry season. Streamflow is generated only if the subsurface storage reservoir is full. The root-zone is treated as a single storage reservoir representing a thin soil layer underlain by deep weathered bedrock (Figure 2), as is common in forested mountainous environments (Amundson et al., 2015; Holbrook et al., 2014; McCormick et al., 2021; Wald et al., 2013). The model does not specify where water is stored within the root-zone or its energy state (e.g., saturated vs. unsaturated). Nor does it mechanistically specify how groundwater produces streamflow at the hillslope-channel boundary, only that water input volumes in excess of the deficit generate flow in the stream.

In our model formulation, storage dynamics evolve annually over three hydrological seasons: a winter wet season when rain enters storage and snow accumulates, a snowmelt season when rain and snowmelt enter storage, and a dry summer season. ET draws from storage at different rates in each season. Starting at the beginning of the wet season, there is a deficit generated by the previous dry season that shrinks with water input during the winter wet season and snowmelt periods (Figure 1d). Once the deficit is reduced to 0, streamflow is generated. When ET exceeds snowmelt and rain in the spring, streamflow stops, and the deficit grows again until the start of the next wet season. Snowmelt runoff emerges as the net water input during the melt season (snowmelt and precipitation less ET) once the deficit has been met. This mass balance results in an expression for spring streamflow (Q [L], normalized by catchment area), in which each of the proposed factors that could impact the relationship between snowpack and streamflow appear as variables:

$$Q = \begin{cases} \text{if } P_w - ET_w > D_{Oct1} : \\ \quad \max(0, SWE - ET_{net} N_{melt}) \\ \text{otherwise:} \\ \quad \max(0\ , SWE - ET_{net} N_{melt} - \\ \qquad\qquad D_{Oct1} + (P_w - ET_w)) \end{cases} \tag{1}$$

where P_w [L] is winter rainfall, ET_w [L] is winter ET, D_{Oct1} [L] is the deficit at the beginning of the wet season, SWE [L] is April 1 snowpack, $ET_{net} = ET_s - P_s$ [L/T] is the mean spring ET rate ET_s less the mean spring precipitation rate P_s, and N_{melt} [T] the length of the snowmelt period. A table of notation is in Table S2 in Supporting Information S1. In Figure 2, $P_r = P_w + P_s$. Both conditions are bounded by zero since streamflow cannot be negative. A negative value for either condition indicates that water demand from ET exceeds water availability from rain and snowmelt, so streamflow must be zero. In Equation 1, all of the hypotheses listed at the end of the introduction for missing snowmelt appear: (a) rain appears in P_w and P_s, (b) snowmelt rate appears in N_{melt} = SWE/m, (c) ET appears in ET_s and ET_w, and (d) the deficit appears as D_{Oct1}. SWE and P_w have long been accounted for in models of snowmelt-driven runoff, so although they appear in Equation 1, neither is the cause of missing snowmelt runoff in 2021. For a full description of the model, see Text S2 in Supporting Information S1.

2.2. A Regression Model for Snowmelt-Driven Runoff

We performed exploratory data analysis to determine which hypotheses listed at the end of the introduction best explain snowmelt runoff at the study sites (Figure 1c). See Text S1 in Supporting Information S1 for details on study sites and site selection criteria, and Text S6 in Supporting Information S1 for additional details on exploratory analysis. To determine which mechanisms have the most explanatory power for deviations from the snowpack-runoff relationship, we developed a multiple linear regression equation at each study site:

$$Q = C_1\ SWE + C_2 P_w + C_3 \frac{D_{Oct1}}{P} + C_4 \frac{ET_{net} N_{melt}}{P} + C_5 \frac{ET_w - P_w}{P} + C_6 \frac{m}{ET_{net}} + C_7, \tag{2}$$

where C_1, …, C_7 are fitted parameters. Note that these drivers are not completely independent of one another. For instance, ET_{net} impacts the size of the fourth and sixth terms. Correlation among variables can reduce interpretability of coefficients in a linear regression model, so we did our best to reduce such correlations, but some correlations remain (see Data supplement in Lapides et al., 2021, the github/zenodo archive). These correlations could lead to incorrect signs or magnitudes in some terms; however, the behavior across all sites should be interpretable if the signs of coefficients are consistent. Linear regressions with fewer parameters (just snowpack and winter rain or the deficit) should not face the same issue.

Each variable other than SWE, m/ET_{net} and P_w is expressed as a fraction of water year precipitation. Expressing variables relative to water year P strengthens the relationship between variables and residuals in the SWE-Q relationship. This normalization also has the effect of minimizing correlation between variables since many model variables are correlated with water year P. In Equation 2, $ET_{net}N_{melt}/P$ and $(ET_w - P_w)/P$ capture effects of variable ET (Hypotheses 3 and 4 in the conceptual runoff model section), $(ET_{nET}N_{melt})/P$ captures effects of variable spring rainfall (Hypothesis 1), m/ET_{net} captures effects of variable snowmelt rate (Hypothesis 2), and D_{Oct1}/P captures effects of variable root-zone storage deficit (Hypothesis 4). Since the relationships among the study variables may not be linear, we also used a random forest model to corroborate the findings of this regression approach; see Text S7 in Supporting Information S1 for additional details. This model does not explicitly account for human impacts, which is appropriate for minimally disturbed basins. However, we also apply this model to 6 water supply basins that are human-impacted under the assumption that actual *ET* will account for some alterations to the landscape, including urbanization, fire, and agriculture.

2.3. Data Sources and Data Processing

Details on site selection criteria for the 15 minimally disturbed basins and site characteristics for all study basins are found in Text S1 in Supporting Information S1.

Streamflow data for all sites other than P300 and B200 were obtained from the National Water Information System (U.S. Geological Survey, 2016) using the package hydrofunctions (https://hydrofunctions.readthedocs.io/en/master/). Streamflow data from P300 and B200 were obtained from the Kings River Experimental watersheds of the US Forest Service Pacific Southwest Research Station (Hunsaker & Safeeq, 2017) for years 2006–2015, and data for 2015–2021 were collected and processed in the same manner as the published 2006–2015 data. Daily SWE was obtained using Snow Data Assimilation System (SNODAS; National Operational Hydrologic Remote Sensing Center, 2000). Precipitation data were obtained from Parameter-elevation Regressions on Independent Slopes Model (PRISM; PRISM Climate Group, 2004). *ET* and temperature data were obtained from PML V2 (Gan et al., 2018; Zhang et al., 2016, 2019) and Moderate Resolution Imaging Spectroradiometer (MODIS; Running et al., 2017). PRISM, MODIS, and PML V2 were accessed via the Google Earth Engine Python API (Gorelick et al., 2017). Evaporative stress index (ESI) data were obtained from ClimateServ (M. Anderson et al., 1997; M. C. Anderson et al., 2007a, 2007b, 2011). ESI provides a measure of *ET* anomalies over time using thermal satellite imagery. A higher ESI indicates a larger positive *ET* anomaly, whereas lower or negative values indicate depressed *ET*. For comparison with root-zone storage deficit, we included soil water storage capacity (Soil Survey Staff, 2019) as processed by McCormick et al. (2021).

For the majority of the study period, we use the PML V2 data set for *ET*. This data set, when combined with PRISM, results in calculated subsurface storage deficits consistent with field measurements (McCormick et al., 2021). Since PML V2 is not yet available through the 2021 water year, we extended the PML V2 data set using MODIS *ET*. We bias-corrected MODIS ET to PML V2 using a basin-specific linear relationship for each study watershed. For most watersheds, the correlation between PML V2 and MODIS ET is strong (median $R^2 >$ 0.4, see Supplementary Code in Lapides et al., 2021).

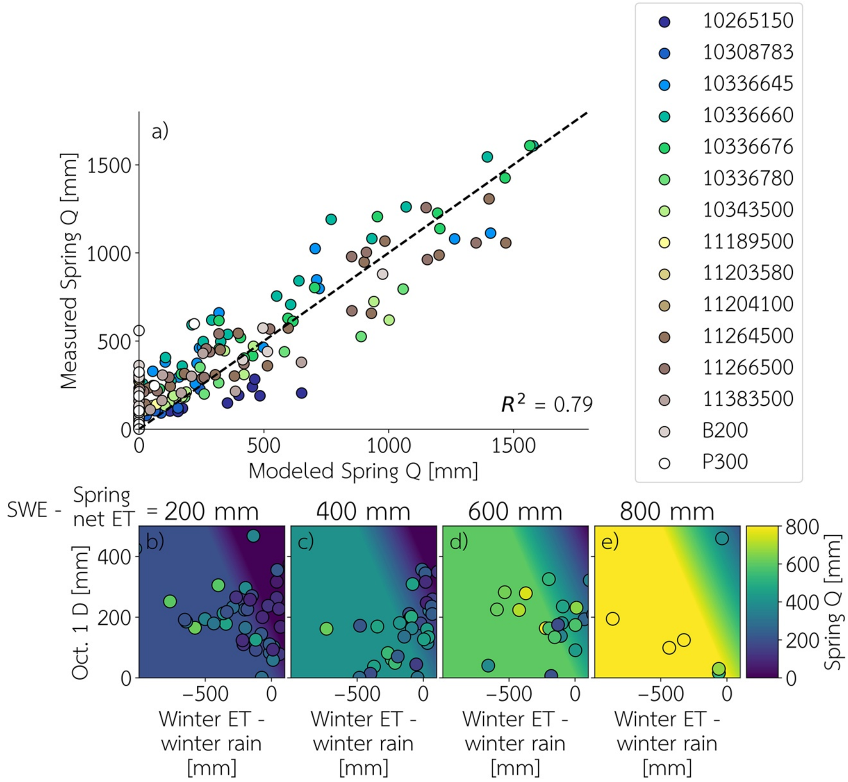

Figure 3. (a) Comparison between measured spring streamflow at minimally disturbed study sites and predicted streamflow for all years based on Equation 1. Legend refers to USGS streamgauge ID or USFS ID number for B200 and P300. (b–e) Heatmaps showing how modeled streamflow varies based on each model parameter. Within each panel: winter evapotranspiration (*ET*)—winter rain increases moving right, and October 1 deficit increases vertically. Moving to the right between panels, April 1 snow water equivalent (SWE)—(spring *ET*—spring rain) increases. Points plotted on heatmaps represent a single water year for a study site and are colored by measured spring streamflow. Points are plotted on the heatmaps if SWE − $ET_{net}N_{melt}$ is within 100 mm of the value labeled for each panel.

Snowmelt rate was calculated from daily SNODAS data as in Barnhart et al. (2016):

$$m = \frac{\Sigma|\min(\Delta SWE_t, 0)|}{\Sigma\Delta_t}, \tag{3}$$

where the numerator is the sum of all daily differences in SWE on days when SWE decreases, and Δ_t is 1 on days when SWE decreases and otherwise 0. See Text S3 in Supporting Information S1 for a description of concordance checks between SNODAS and PRISM.

The root-zone storage deficit was calculated following Wang-Erlandsson et al. (2016) and Dralle et al. (2021). The only difference here is that instead of using only precipitation and *ET* (Wang-Erlandsson et al., 2016) or approximating information about snow using snow cover (Dralle et al., 2021), we used SNODAS data directly to represent accumulation and melt of snowpack. For a full description of deficit calculations, see Text S4 in Supporting Information S1. For a justification of why this deficit is specifically a "root-zone" storage deficit, refer to Text S9 in Supporting Information S1.

3. Results

The mass balance model of root-zone storage (Equation 1) accurately predicts measured spring streamflow (Nash-Sutcliffe Efficiency [NSE] = 0.79, see Figure 3a) at 15 minimally disturbed sites in the Sierra Nevada (gray sites in Figure 1c). Panels (b–e) plot these same predictions, showing scatter points colored by actual spring streamflow against heatmaps generated from the mass balance model. Good model performance despite a lack of

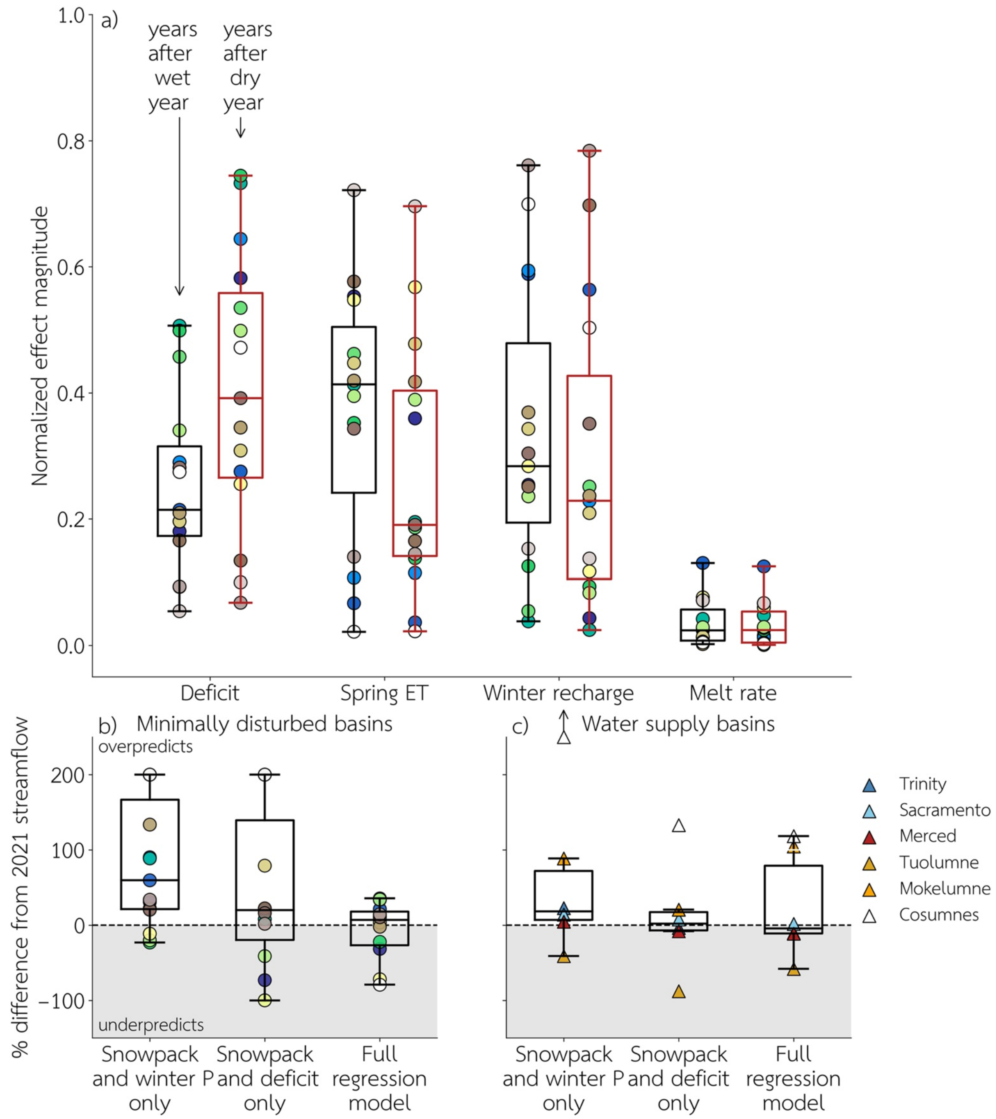

Figure 4. (a) Normalized effect magnitude of each variable included in the multiple linear regression for snowmelt runoff at all sites, comparing the set of years following wet years to years following dry years. Snowpack and winter rainfall (excluded from plot) are consistently the most important variables. Variable names are described for the water balance feature they represent, but deficit, spring net evapotranspiration (*ET*), and winter recharge are relative to water year precipitation, and melt rate is relative to spring net *ET*. Box and whisker plot shows median value across all minimally disturbed sites. Effect size is the coefficient for a given variable multiplied by the median absolute value of the variable for years following wet (black) or dry (red) years. Normalization is achieved by scaling effect sizes for each site so that absolute values sum to 1. Performance of regression models in 2021 at (b) 15 minimally disturbed and (c) 6 water supply basins. Legend for panels (a and b) is the same as for Figure 3a.

tunable parameters suggests that the model captures the primary mechanisms for spring streamflow generation at the study sites.

3.1. Root-Zone Storage Deficit Is Important for Determining Runoff From Snowpack

We regressed spring runoff (April-July, proxy for snowmelt runoff) on the variables identified in the storage-based modeling framework (Equation 2) at the 15 minimally disturbed sites to quantitatively rank the importance of different physical drivers of snowmelt runoff generation during years following both wet (above 75th percentile of annual precipitation) and dry (below 25th percentile of annual precipitation) years (Figure 4a). Model outcomes in both wet and dry years are most sensitive to snowpack and winter rainfall, the two parameters included in the forecasting model used as an example in this study. Assuming first-order effects are captured by the model, the remaining variables (shown in Figure 4a) must explain performance failure in 2021. Of these four variables, only the effect size of the deficit is larger in years following dry years than wet years, and it is substantially larger, making it by far the most important term in years following dry years, even larger than winter rainfall (not shown). This suggests that large deficits generated during dry years play an essential role in reducing snowmelt runoff in the following year. See Tables S5 and S6 in Supporting Information S1 for effect sizes for all variables at all sites on wet and dry years.

With rare exceptions, the sign for each effect size matches the expected sign based on hypothesized model mechanisms at all sites (see Tables S5 and S6 in Supporting Information S1), providing further evidence for the proposed conceptual framework. No more than two sites show an unexpected sign for any parameter except for the melt rate, which has an unexpected sign at four sites, and (surprisingly) winter rain, which has an unexpected sign at three sites. Given the melt rate's small effect sizes and unexpected effect signs, we conclude that melt rate is relatively insignificant in comparison to other explanatory variables. The same conclusion cannot be drawn for winter rain because its effect size is very large. Instead, we suggest that at those sites with an unexpected sign for winter rainfall there may be either (a) a negative relationship between total precipitation or SWE and winter rainfall during the study period that confounds interpretation of the winter rainfall coefficient or (b) errors in precipitation from PRISM due to the small size of the catchments. The median NSE value for multiple linear regression models across the study sites is 0.92, and median mean absolute error (MAE) from leave-one-out cross-validation is 89 mm.

We also trained a single random forest model to predict spring streamflow at all sites based on the same set of input parameters (model performance NSE = 0.98, MAE = 87 mm) since a linear model may not account for complex interactions between the hydrologic processes used in the regression. Results from the random forest analysis also support the hypothesized mechanisms (see Figure S4 in Supporting Information S1); contribution of parameters to model outputs as measured by feature importance confirms that October 1 deficit and spring net *ET* are important drivers of snowmelt runoff, whereas the melt rate is less important. See Text S7 in Supporting Information S1 for more details.

3.2. Using Deficits Increases Predictive Power of Forecasting Models Following Drought

A linear regression model using snowpack and winter rainfall (Figure 1a) replicates the 2021 "missing" streamflow phenomenon with a similar magnitude of error in 2021 (California Department of Water Resources, 2021). Linear regressions of this type have been used by the California Department of Water Resources (personal communication with Sean de Guzman, chief of the California Department of Water Resources Snow Surveys and Water Supply Forecasting Section) and in research applications exploring snowpack-runoff relationships (Godsey et al., 2014). By including a term representing the deficit (linear regression using only snowpack and deficit) rather than winter rainfall, model performance on years following dry years improves from a median of NSE = 0.42 to a median NSE of 0.62 (median MAE from leave-one-out cross-validation improves from 99 to 72 mm). On years following wet years, performance is lower in the model that replaces rainfall with the deficit (NSE of 0.55 compared to 0.85, MAE of 112 mm compared to 45 mm) since rainfall is a more important predictor in those years. However, when both rainfall and deficit are included in the full regression model, performance is very good on years following wet years (NSE = 0.86, MAE = 56 mm). For site-specific details, see Tables S7 and S8 in Supporting Information S1.

When focusing on the 2021 water year, gains in forecast skill are striking. Figure 4b shows predictions for 2021 streamflow at the minimally disturbed sites using the full multiple linear regression model, snowpack and deficit only, and snowpack and winter rain only. Each regression model is trained on data from the full study period and assessed using MAE from leave-one-out cross-validation and NSE for all years, years following wet years, and years following dry years. Using only snowpack and rainfall, the model over-predicts the 2021 streamflow at all minimally disturbed sites by a median of 60%. Using the full regression model, median streamflow is only over-predicted by 7%, and with snowpack and deficit it is over-predicted by only 20%.

We tested our model on minimally disturbed basins. However, given that the deficit is calculated using remotely sensed *ET*, it should be sensitive to spatial variation in land-cover or forms of disturbance, such as fire, that are known to impact patterns of plant water use (Boisramé et al., 2017; Lowman & Barros, 2019; Pausas &

Keeley, 2019; Renninger et al., 2013). This suggests our model may be applicable to larger and more complex basins. We therefore also applied the model to six watersheds central to California's water supply (green basins in Figure 1c and Text S1 in Supporting Information S1 for additional site information). As shown in Figure 4c, adding a term to a linear regression model to represent the deficit improves error in prediction of 2021 streamflow from a median of 18% to a median of 2% overprediction. With the full regression, streamflow is underpredicted by a median of 4%. The sum of errors across the water supply basins is reduced from 34% to 3% with the inclusion of the deficit. Therefore, despite noise introduced by fire and logging legacies, incorporating the root-zone storage deficit into models for spring streamflow from snowpack substantially improves model performance for water resources-relevant forecasting, especially following dry years.

4. Discussion and Conclusions

Large drought-induced root-zone storage deficits at the start of the 2021 wet season led to the "missing" streamflow phenomenon. Adding a term to describe root-zone storage deficit decreased total overprediction of 2021 snowmelt runoff in a linear regression model from 60% to 20% across minimally disturbed study basins and from 18% to 2% across water supply basins, an essential improvement for water resources management. Not only does October 1 deficit drive reductions in streamflow following dry years, but it can be quantified prior to the snowmelt season for the purpose of improved snowmelt runoff forecasting. Results demonstrate that: (a) the deficit is an essential quantity for predicting snowmelt runoff in years following dry years; and (b) the quantification of the deficit used in this study captures the signal of time-varying subsurface moisture conditions. Together, these results indicate that a management model including snowpack, winter rainfall, and the deficit would have greater skill in predicting snowmelt runoff, particularly in years following drought.

Managers and researchers have long recognized the importance of subsurface moisture conditions for subsequent runoff (Arkley, 1981; Bales et al., 2011; Goulden & Bales, 2019; Grindley, 1960; Hahm et al., 2021; Jones & Graham, 1993; Klos et al., 2018; Lewis & Burgy, 1964; M. Anderson et al., 1995; McCormick et al., 2021; Miller et al., 2010; Rempe & Dietrich, 2018; Rose et al., 2003; Sayama et al., 2011); however, incorporating root-zone water storage dynamics into forecasting presents a challenge. This is due to both the limited available data on water storage in weathered bedrock, as well as the challenge of understanding interactions between different drivers of root-zone dynamics. The presented model quantitatively captures the expected importance of subsurface moisture conditions for runoff forecasting, providing a low-complexity solution to the problem of runoff prediction, without reliance on water storage parameters that are poorly constrained at large spatial scales (Dralle et al., 2021; Wang-Erlandsson et al., 2016). The model captures snowmelt runoff well following dry years, which is essential given the projected increase in "weather whiplash," that is, alternation between extreme wet and dry years (Persad et al., 2020).

While simple, the good performance of our mass-balance model suggests that first-order hydrological behavior is captured. A more complex model may capture additional site-specific nuance, but a simple model provides high-level insight into the drivers of changes in hydrological function. A further implication of good performance of our mass balance model is that runoff generation in the Sierra is not highly dependent on infiltration-excess overland flow processes, which is not included as a runoff process in our model and should be relatively insensitive to root-zone storage deficits (Castillo et al., 2003). Instead, the agreement between the presented model and data supports the hypothesis that replenishment of root-zone storage deficits is required for significant runoff generation to occur, which is more consistent with saturation overland (Dunne & Black, 1970) or subsurface (Freeze, 1972) flow generation mechanisms. Additionally, since the data used in this study are gridded, the spatial distribution of precipitation and ET are neglected. Thus, the good performance of our model also suggests that heterogeneity in these fluxes may not be of first-order importance for spring streamflow generation at the study sites.

Climate change is impacting the reliability and predictability of water supply in many ways, one of which is post-drought reductions in expected snowmelt runoff. Root-zone storage deficits provide a means of monitoring changing conditions, but operationalizing deficits in real-time requires the development of frequently updated, reliable, large-scale ET, and precipitation data sets. Multiple data products are being developed and tested in the community to support urgent needs for research and management applications (Guo et al., 2022; Mazzoleni et al., 2019), and the present study provides yet more motivation to continue honing these essential data sets.

Data Availability Statement

Data and code generated for this publication are available in an online data repository, https://github.com/lapidesd/CA_missing_freshet (Lapides et al., 2021). Raster maps of percentiles of April 1 snow water equivalent are available at https://www.hydroshare.org/resource/4b940b8593a4416e954a47bbbc58c568/ (Lapides et al., 2022).

Acknowledgments
The authors would like to thank Sean de Guzman, chief of the California Department of Water Resources Snow Surveys and Water Supply Forecasting Section, for providing insight into how runoff is forecast in California. Funding was provided by the Simon Fraser University, a Natural Sciences and Engineering Research Council of Canada Discovery Grant, the Canada Foundation for Innovation, and the USDA Forest Service Pacific Southwest Research Station with funds administered by Oak Ridge Institute for Science and Education (ORISE).

References

Amundson, R., Heimsath, A., Owen, J., Yoo, K., & Dietrich, W. E. (2015). Hillslope soils and vegetation. *Geomorphology*, *234*, 122–132. https://doi.org/10.1016/j.geomorph.2014.12.031

Anderson, M., Graham, R., Alyanakian, G., & Martynn, D. (1995). Late summer water status of soils and weathered bedrock in a giant sequoia grove. *Soil Science*, *160*(6), 415–422. https://doi.org/10.1097/00010694-199512000-00007

Anderson, M., Norman, J., Diak, G., Kustas, W., & Mecikalski, J. (1997). A two-source time-integrated model for estimating surface fluxes using thermal infrared remote sensing. *Remote Sensing of Environment*, *60*(2), 195–216. https://doi.org/10.1016/s0034-4257(96)00215-5

Anderson, M. C., Hain, C., Wardlow, B., Pimstein, A., Mecikalski, J. R., & Kustas, W. P. (2011). Evaluation of drought indices based on thermal remote sensing of evapotranspiration over the continental United States. *Journal of Climate*, *24*(8), 2025–2044. https://doi.org/10.1175/2010jcli3812.1

Anderson, M. C., Norman, J. M., Mecikalski, J. R., Otkin, J. A., & Kustas, W. P. (2007a). A climatological study of evapotranspiration and moisture stress across the continental United States based on thermal remote sensing: 1. Model formulation. *Journal of Geophysical Research*, *112*(D10), D10117. https://doi.org/10.1029/2006jd007506

Anderson, M. C., Norman, J. M., Mecikalski, J. R., Otkin, J. A., & Kustas, W. P. (2007b). A climatological study of evapotranspiration and moisture stress across the continental United States based on thermal remote sensing: 2. Surface moisture climatology. *Journal of Geophysical Research*, *112*(D11), D11112. https://doi.org/10.1029/2006jd007507

Arkley, R. J. (1981). Soil moisture use by mixed conifer forest in a summer-dry climate. *Soil Science Society of America Journal*, *45*(2), 423–427. https://doi.org/10.2136/sssaj1981.03615995004500020037x

Avanzi, F., Rungee, J., Maurer, T., Bales, R., Ma, Q., Glaser, S., & Conklin, M. (2020). Climate elasticity of evapotranspiration shifts the water balance of Mediterranean climates during multi-year droughts. *Hydrology and Earth System Sciences*, *24*(9), 4317–4337. https://doi.org/10.5194/hess-24-4317-2020

Bales, R. C., Hopmans, J. W., O'Geen, A. T., Meadows, M., Hartsough, P. C., Kirchner, P., et al. (2011). Soil moisture response to snowmelt and rainfall in a Sierra Nevada mixed-conifer forest. *Vadose Zone Journal*, *10*(3), 786–799. https://doi.org/10.2136/vzj2011.0001

Barnhart, T. B., Molotch, N. P., Livneh, B., Harpold, A. A., Knowles, J. F., & Schneider, D. (2016). Snowmelt rate dictates streamflow. *Geophysical Research Letters*, *43*(15), 8006–8016. https://doi.org/10.1002/2016gl069690

Bayazit, M. (2015). Nonstationarity of hydrological records and recent trends in trend analysis: A state-of-the-art review. *Environmental Processes*, *2*(3), 527–542. https://doi.org/10.1007/s40710-015-0081-7

Boisramé, G., Thompson, S., Collins, B., & Stephens, S. (2017). Managed wildfire effects on forest resilience and water in the Sierra Nevada. *Ecosystems*, *20*(4), 717–732. https://doi.org/10.1007/s10021-016-0048-1

Boon, S. (2009). Snow ablation energy balance in a dead forest stand. *Hydrological Processes: An International Journal*, *23*(18), 2600–2610. https://doi.org/10.1002/hyp.7246

California Department of Water Resources. (2021). DWR bulletin-120 forecast performance, water year 2021. Retrieved from https://tableau.cnra.ca.gov/t/DWR_Snow_WSFcast/views/WY2021Performance/Dashboard1?%3Adisplay_count=n%26%3Aembed=y%26%3AisGuestRedirectFromVizportal=y%26%3Aorigin%20=viz_share_link%26%3AshowAppBanner=false%26%3AshowVizHome=n

Canon, G. (2021). *'Truly an emergency': How drought returned to California – And what lies ahead*. Guardian. Retrieved from https://www.theguardian.com/us-news/2021/jun/07/california-drought-oregon-west-climate-change

Castillo, V., Gomez-Plaza, A., & Martınez-Mena, M. (2003). The role of antecedent soil water content in the runoff response of semiarid catchments: A simulation approach. *Journal of Hydrology*, *284*(1–4), 114–130. https://doi.org/10.1016/s0022-1694(03)00264-6

DeWalle, D. R., & Rango, A. (2008). *Principles of snow hydrology*. Cambridge University Press.

Dralle, D. N., Hahm, W. J., Chadwick, K. D., McCormick, E., & Rempe, D. M. (2021). Accounting for snow in the estimation of root zone water storage capacity from precipitation and evapotranspiration fluxes. *Hydrology and Earth System Sciences*, *25*(5), 2861–2867. https://doi.org/10.5194/hess-25-2861-2021

Dunne, T., & Black, R. D. (1970). An experimental investigation of runoff production in permeable soils. *Water Resources Research*, *6*(2), 478–490. https://doi.org/10.1029/wr006i002p00478

Entekhabi, D., Njoku, E. G., O'Neill, P. E., Kellogg, K. H., Crow, W. T., Edelstein, W. N., et al. (2010). The soil moisture active passive (SMAP) mission. *Proceedings of the IEEE*, *98*(5), 704–716. https://doi.org/10.1109/JPROC.2010.2043918

Fowler, K., Knoben, W., Peel, M., Peterson, T., Ryu, D., Saft, M., et al. (2020). Many commonly used rainfall-runoff models lack long, slow dynamics: Implications for runoff projections. *Water Resources Research*, *56*(5), e2019WR025286. https://doi.org/10.1029/2019wr025286

Fowler, K. J., Coxon, G., Freer, J. E., Knoben, W. J., Peel, M. C., Wagener, T., et al. (2021). Towards more realistic runoff projections by removing limits on simulated soil moisture deficit. *Journal of Hydrology*, *600*, 126505. https://doi.org/10.1016/j.jhydrol.2021.126505

Freeze, R. A. (1972). Role of subsurface flow in generating surface runoff: 1. Base flow contributions to channel flow. *Water Resources Research*, *8*(3), 609–623. https://doi.org/10.1029/wr008i003p00609

Gan, R., Zhang, Y., Shi, H., Yang, Y., Eamus, D., Cheng, L., et al. (2018). Use of satellite leaf area index estimating evapotranspiration and gross assimilation for Australian ecosystems. *Ecohydrology*, *11*(5), e1974. https://doi.org/10.1002/eco.1974

Garcia-Barreda, S., & Camarero, J. J. (2020). Tree ring and water deficit indices as indicators of drought impact on black truffle production in Spain. *Forest Ecology and Management*, *475*, 118438. https://doi.org/10.1016/j.foreco.2020.118438

Geruo, A., Velicogna, I., Kimball, J. S., Du, J., Kim, Y., Colliander, A., & Njoku, E. (2017). Satellite-observed changes in vegetation sensitivities to surface soil moisture and total water storage variations since the 2011 Texas drought. *Environmental Research Letters*, *12*(5), 054006. https://doi.org/10.1088/1748-9326/aa6965

Godsey, S. E., Kirchner, J. W., & Tague, C. L. (2014). Effects of changes in winter snowpacks on summer low flows: Case studies in the Sierra Nevada, California, USA. *Hydrological Processes*, *28*(19), 5048–5064. https://doi.org/10.1002/hyp.9943

Gorelick, N., Hancher, M., Dixon, M., Ilyushchenko, S., Thau, D., & Moore, R. (2017). Google Earth Engine: Planetary-scale geospatial analysis for everyone. *Remote Sensing of Environment*, *202*, 18–27. https://doi.org/10.1016/j.rse.2017.06.031

Goulden, M. L., & Bales, R. C. (2019). California forest die-off linked to multi-year deep soil drying in 2012–2015 drought. *Nature Geoscience*, *12*(8), 632–637. https://doi.org/10.1038/s41561-019-0388-5

Grindley, J. (1960). Calculated soil moisture deficits in the dry summer of 1959 and forecast dates of first appreciable runoff. *International Association of Scientific Hydrology*, 109–120.

Guo, X., Wu, Z., He, H., & Xu, Z. (2022). Evaluating the potential of different evapotranspiration datasets for distributed hydrological model calibration. *Remote Sensing*, *14*(3), 629. https://doi.org/10.3390/rs14030629

Hahm, W. J., Dralle, D., Rempe, D., Bryk, A., Thompson, S., Dawson, T., & Dietrich, W. (2019). Low subsurface water storage capacity relative to annual rainfall decouples Mediterranean plant productivity and water use from rainfall variability. *Geophysical Research Letters*, *46*(12), 6544–6553. https://doi.org/10.1029/2019gl083294

Hahm, W. J., Dralle, D. N., Sanders, M., Bryk, A. B., Fauria, K. E., Huang, M.-H., et al. (2021). Bedrock vadose zone storage dynamics under extreme drought: Consequences for plant water availability, recharge, and runoff. *Water Resources Research*, *58*(4), e2021WR031781. https://doi.org/10.1002/essoar.10509661.2

Hahm, W. J., Rempe, D., Dralle, D., Dawson, T., & Dietrich, W. (2020). Oak transpiration drawn from the weathered bedrock vadose zone in the summer dry season. *Water Resources Research*, *56*(11), e2020WR027419. https://doi.org/10.1029/2020wr027419

Hamlet, A. F., Mote, P. W., Clark, M. P., & Lettenmaier, D. P. (2007). Twentieth-century trends in runoff, evapotranspiration, and soil moisture in the western United States. *Journal of Climate*, *20*(8), 1468–1486. https://doi.org/10.1175/jcli4051.1

Harpold, A. A., Sutcliffe, K., Clayton, J., Goodbody, A., & Vazquez, S. (2017). Does including soil moisture observations improve operational streamflow forecasts in snow-dominated watersheds? *JAWRA Journal of the American Water Resources Association*, *53*(1), 179–196. https://doi.org/10.1111/1752-1688.12490

Hawkins, T., & Ellis, A. (2010). The dependence of streamflow on antecedent subsurface moisture in an arid climate. *Journal of Arid Environments*, *74*(1), 75–86. https://doi.org/10.1016/j.jaridenv.2009.07.003

Hoerling, M., & Eischeid, J. (2007). Past peak water in the southwest. *Southwest Hydrology*, *6*(1), 18–19.

Holbrook, W. S., Riebe, C. S., Elwaseif, M., Hayes, J. L., Basler-Reeder, K., Harry, D., et al. (2014). Geophysical constraints on deep weathering and water storage potential in the Southern Sierra Critical Zone Observatory. *Earth Surface Processes and Landforms*, *39*(3), 366–380. https://doi.org/10.1002/esp.3502

Hunsaker, C. T., & Safeeq, M. (2017). Kings river experimental watersheds stream discharge. https://doi.org/10.2737/RDS-2017-0037

Ichii, K., Wang, W., Hashimoto, H., Yang, F., Votava, P., Michaelis, A. R., & Nemani, R. R. (2009). Refinement of rooting depths using satellite-based evapotranspiration seasonality for ecosystem modeling in California. *Agricultural and Forest Meteorology*, *149*(11), 1907–1918. https://doi.org/10.1016/j.agrformet.2009.06.019

Immerzeel, W. W., Lutz, A., Andrade, M., Bahl, A., Biemans, H., Bolch, T., et al. (2020). Importance and vulnerability of the world's water towers. *Nature*, *577*(7790), 364–369. https://doi.org/10.1038/s41586-019-1822-y

Jones, D., & Graham, R. (1993). Water-holding characteristics of weathered granitic rock in chaparral and forest ecosystems. *Soil Science Society of America Journal*, *57*(1), 256–261. https://doi.org/10.2136/sssaj1993.03615995005700010044x

Klos, P. Z., Goulden, M. L., Riebe, C. S., Tague, C. L., O'Geen, A. T., Flinchum, B. A., et al. (2018). Subsurface plant-accessible water in mountain ecosystems with a Mediterranean climate. *Wiley Interdisciplinary Reviews: Water*, *5*(3), e1277. https://doi.org/10.1002/wat2.1277

Knight, D. H., Yavitt, J. B., & Joyce, G. D. (1991). Water and nitrogen outflow from lodgepole pine forest after two levels of tree mortality. *Forest Ecology and Management*, *46*(3–4), 215–225. https://doi.org/10.1016/0378-1127(91)90233-l

Koster, R. D., Mahanama, S. P., Livneh, B., Lettenmaier, D. P., & Reichle, R. H. (2010). Skill in streamflow forecasts derived from large-scale estimates of soil moisture and snow. *Nature Geoscience*, *3*(9), 613–616. https://doi.org/10.1038/ngeo944

Lapides, D. A., Hahm, W. J., Rempe, D. M., Dralle, D. (2022). *April 1 SWE spatial percentiles using SNODAS for the contiguous USA*. HydroShare. https://doi.org/10.4211/hs.4b940b8593a4416e954a47bbbc58c568

Lapides, D. A., Hahm, W. J., Rempe, D. M., & Dralle, D. N. (2021). Supplementary code and data for: Root zone storage deficits mediate the production of streamflow from snowmelt. https://doi.org/10.5281/zenodo.7062803

Lewis, D., & Burgy, R. H. (1964). The relationship between oak tree roots and groundwater in fractured rock as determined by tritium tracing. *Journal of Geophysical Research*, *69*(12), 2579–2588. https://doi.org/10.1029/jz069i012p02579

Li, X., Zhang, Q., & Ye, X. (2013). Effects of spatial information of soil physical properties on hydrological modeling based on a distributed hydrological model. *Chinese Geographical Science*, *23*(2), 182–193. https://doi.org/10.1007/s11769-013-0599-4

Livneh, B., & Badger, A. M. (2020). Drought less predictable under declining future snowpack. *Nature Climate Change*, *10*(5), 452–458. https://doi.org/10.1038/s41558-020-0754-8

Lowman, L., & Barros, A. P. (2019). Fire-induced canopy changes alter plant water, energy and carbon relations for coastal plains forests in the southeast us. In *AGU Fall Meeting Abstracts* (Vol. 2019, pp. B53H–2500).

Mahanama, S., Livneh, B., Koster, R., Lettenmaier, D., & Reichle, R. (2012). Soil moisture, snow, and seasonal streamflow forecasts in the United States. *Journal of Hydrometeorology*, *13*(1), 189–203. https://doi.org/10.1175/jhm-d-11-046.1

Massari, C., Avanzi, F., Bruno, G., Gabellani, S., Penna, D., & Camici, S. (2022). Evaporation enhancement drives the European water-budget deficit during multi-year droughts. *Hydrology and Earth System Sciences*, *26*(6), 1527–1543. https://doi.org/10.5194/hess-26-1527-2022

Mazzoleni, M., Brandimarte, L., & Amaranto, A. (2019). Evaluating precipitation datasets for large-scale distributed hydrological modelling. *Journal of Hydrology*, *578*, 124076. https://doi.org/10.1016/j.jhydrol.2019.124076

McCormick, E. L., Dralle, D. N., Hahm, W. J., Tune, A. K., Schmidt, L. M., Chadwick, K. D., & Rempe, D. M. (2021). Widespread woody plant use of water stored in bedrock. *Nature*, *597*(7875), 225–229. https://doi.org/10.1038/s41586-021-03761-3

McDonnell, J. J., Spence, C., Karran, D. J., Ilja van Meerveld, H., & Harman, C. (2021). *Fill-and-spill: A process description of runoff generation at the scale of the beholder* (p. e2020WR027514). Water Resources Research.

Miller, G. R., Chen, X., Rubin, Y., Ma, S., & Baldocchi, D. D. (2010). Groundwater uptake by woody vegetation in a semiarid oak savanna. *Water Resources Research*, *46*(10), 2009WR008902. https://doi.org/10.1029/2009wr008902

Milly, P. C., & Dunne, K. A. (2020). Colorado river flow dwindles as warming-driven loss of reflective snow energizes evaporation. *Science*, *367*(6483), 1252–1255. https://doi.org/10.1126/science.aay9187

National Operational Hydrologic Remote Sensing Center. (2000). *Snow Data Assimilation System (SNODAS) data products at NSIDC, version 1*. NSIDC: National Snow and Ice Data Center. https://doi.org/10.7265/N5TB14TC

Paltineanu, C., Mihailescu, I., Prefac, Z., Dragota, C., Vasenciuc, F., & Claudia, N. (2009). Combining the standardized precipitation index and climatic water deficit in characterizing droughts: A case study in Romania. *Theoretical and Applied Climatology*, *97*(3), 219–233. https://doi.org/10.1007/s00704-008-0061-1

Pausas, J. G., & Keeley, J. E. (2019). Wildfires as an ecosystem service. *Frontiers in Ecology and the Environment*, *17*(5), 289–295. https://doi.org/10.1002/fee.2044

Penna, D., Tromp-van Meerveld, H., Gobbi, A., Borga, M., & Dalla Fontana, G. (2011). The influence of soil moisture on threshold runoff generation processes in an alpine headwater catchment. *Hydrology and Earth System Sciences*, *15*(3), 689–702. https://doi.org/10.5194/hess-15-689-2011

Penna, D., van Meerveld, H. J., Oliviero, O., Zuecco, G., Assendelft, R., Dalla Fontana, G., & Borga, M. (2015). Seasonal changes in runoff generation in a small forested mountain catchment. *Hydrological Processes*, *29*(8), 2027–2042. https://doi.org/10.1002/hyp.10347

Persad, G. G., Swain, D. L., Kouba, C., & Ortiz-Partida, J. P. (2020). Inter-model agreement on projected shifts in California hydroclimate characteristics critical to water management. *Climatic Change*, *162*(3), 1493–1513. https://doi.org/10.1007/s10584-020-02882-4

PRISM Climate Group. (2004). Prism rainfall dataset. Retrieved from http://prism.oregonstate.edu

Pugh, E., & Small, E. (2012). The impact of pine beetle infestation on snow accumulation and melt in the headwaters of the Colorado River. *Ecohydrology*, *5*(4), 467–477. https://doi.org/10.1002/eco.239

Rempe, D. M., & Dietrich, W. E. (2018). Direct observations of rock moisture, a hidden component of the hydrologic cycle. *Proceedings of the National Academy of Sciences*, *115*(11), 2664–2669. https://doi.org/10.1073/pnas.1800141115

Renninger, H. J., Clark, K. L., Skowronski, N., & Schäfer, K. V. (2013). Effects of a prescribed fire on water use and photosynthetic capacity of pitch pines. *Trees*, *27*(4), 1115–1127. https://doi.org/10.1007/s00468-013-0861-5

Roche, J. W., Ma, Q., Rungee, J., & Bales, R. C. (2020). Evapotranspiration mapping for forest management in California's Sierra Nevada. *Frontiers in Forests and Global Change*, *3*, 69. https://doi.org/10.3389/ffgc.2020.00069

Rogers, P. (2021). *Where did Sierra snow go this spring? Not into California rivers and water supplies*. The Mercury News.

Rose, K., Graham, R., & Parker, D. (2003). Water source utilization by *Pinus jeffreyi* and *Arctostaphylos patula* on thin soils over bedrock. *Oecologia*, *134*(1), 46–54. https://doi.org/10.1007/s00442-002-1084-4

Running, S., Mu, Q., & Zhao, M. (2017). MOD16A2 MODIS/Terra net evapotranspiration 8-day L4 global 500m sin grid v006 [Dataset]. NASA EOSDIS Land Processes DAAC. https://doi.org/10.5067/MODIS/MOD16A2.006

Sayama, T., McDonnell, J. J., Dhakal, A., & Sullivan, K. (2011). How much water can a watershed store? *Hydrological Processes*, *25*(25), 3899–3908. https://doi.org/10.1002/hyp.8288

Soil Survey Staff. (2019). *Gridded National Soil Survey Geographic (gNATSGO) database for the conterminous United States*. USDA. Retrieved from https://nrcs.app.box.com/v/soils

Sproles, E., Leibowitz, S., Reager, J., Wigington, P., Jr., Famiglietti, J., & Patil, S. (2015). GRACE storage-runoff hystereses reveal the dynamics of regional watersheds. *Hydrology and Earth System Sciences*, *19*(7), 3253–3272. https://doi.org/10.5194/hess-19-3253-2015

Thomas, A. C., Reager, J. T., Famiglietti, J. S., & Rodell, M. (2014). A grace-based water storage deficit approach for hydrological drought characterization. *Geophysical Research Letters*, *41*(5), 1537–1545. https://doi.org/10.1002/2014gl059323

U.S. Geological Survey. (2016). National Water Information System data available on the World Wide Web (USGS Water Data for the Nation). Retrieved from http://waterdata.usgs.gov/nwis/

Vano, J. A. (2020). Implications of losing snowpack. *Nature Climate Change*, *10*(5), 388–390. https://doi.org/10.1038/s41558-020-0769-1

Wald, J. A., Graham, R. C., & Schoeneberger, P. J. (2013). Distribution and properties of soft weathered bedrock at ≤ 1 m depth in the contiguous United States. *Earth Surface Processes and Landforms*, *38*(6), 614–626. https://doi.org/10.1002/esp.3343

Wang-Erlandsson, L., Bastiaanssen, W. G., Gao, H., Jägermeyr, J., Senay, G. B., Van Dijk, A. I., et al. (2016). Global root zone storage capacity from satellite-based evaporation. *Hydrology and Earth System Sciences*, *20*(4), 1459–1481. https://doi.org/10.5194/hess-20-1459-2016

Wrzesien, M. L., Durand, M. T., Pavelsky, T. M., Howat, I. M., Margulis, S. A., & Huning, L. S. (2017). Comparison of methods to estimate snow water equivalent at the mountain range scale: A case study of the California Sierra Nevada. *Journal of Hydrometeorology*, *18*(4), 1101–1119. https://doi.org/10.1175/jhm-d-16-0246.1

Zhang, Y., Kong, D., Gan, R., Chiew, F. H., McVicar, T. R., Zhang, Q., & Yang, Y. (2019). Coupled estimation of 500 m and 8-day resolution global evapotranspiration and gross primary production in 2002–2017. *Remote Sensing of Environment*, *222*, 165–182. https://doi.org/10.1016/j.rse.2018.12.031

Zhang, Y., Peña-Arancibia, J. L., McVicar, T. R., Chiew, F. H., Vaze, J., Liu, C., et al. (2016). Multi-decadal trends in global terrestrial evapotranspiration and its components. *Scientific Reports*, *6*(1), 1–12. https://doi.org/10.1038/srep19124

References From the Supporting Information

Botter, G., Porporato, A., Daly, E., Rodriguez-Iturbe, I., & Rinaldo, A. (2007). Probabilistic characterization of base flows in river basins: Roles of soil, vegetation, and geomorphology. *Water Resources Research*, *43*(6), W06404. https://doi.org/10.1029/2006wr005397

Byer, S., & Jin, Y. (2017). Detecting drought-induced tree mortality in Sierra Nevada forests with time series of satellite data. *Remote Sensing*, *9*(9), 929. https://doi.org/10.3390/rs9090929

CAL FIRE. (2019). Timber harvest plans (THPs) – CAL FIRE [ds816]. Retrieved from https://map.dfg.ca.gov/metadata/ds0816.html

Cui, G., Ma, Q., & Bales, R. (2022). Assessing multi-year-drought vulnerability in dense Mediterranean-climate forests using water-balance-based indicators. *Journal of Hydrology*, *606*, 127431. https://doi.org/10.1016/j.jhydrol.2022.127431

Dettinger, M. D., Ralph, F. M., Das, T., Neiman, P. J., & Cayan, D. R. (2011). Atmospheric rivers, floods and the water resources of California. *Water*, *3*(2), 445–478. https://doi.org/10.3390/w3020445

Diffenbaugh, N. S., Swain, D. L., & Touma, D. (2015). Anthropogenic warming has increased drought risk in California. *Proceedings of the National Academy of Sciences*, *112*(13), 3931–3936. https://doi.org/10.1073/pnas.1422385112

Falcone, J. (2017). *US Geological Survey GAGES-II time series data from consistent sources of land use, water use, agriculture, timber activities, dam removals, and other historical anthropogenic influences: US Geological Survey data release*. US Geological Survey data release.

Fettig, C. J., Mortenson, L. A., Bulaon, B. M., & Foulk, P. B. (2019). Tree mortality following drought in the central and southern Sierra Nevada, California, us. *Forest Ecology and Management*, *432*, 164–178. https://doi.org/10.1016/j.foreco.2018.09.006

Griffin, D., & Anchukaitis, K. J. (2014). How unusual is the 2012–2014 California drought? *Geophysical Research Letters*, *41*(24), 9017–9023. https://doi.org/10.1002/2014gl062433

Guarín, A., & Taylor, A. H. (2005). Drought triggered tree mortality in mixed conifer forests in Yosemite National Park, California, USA. *Forest Ecology and Management*, *218*(1–3), 229–244. https://doi.org/10.1016/j.foreco.2005.07.014

Handwerger, A. L., Fielding, E. J., Huang, M.-H., Bennett, G. L., Liang, C., & Schulz, W. H. (2019). Widespread initiation, reactivation, and acceleration of landslides in the northern California Coast Ranges due to extreme rainfall. *Journal of Geophysical Research: Earth Surface*, *124*(7), 1782–1797. https://doi.org/10.1029/2019jf005035

Hatchett, B. J., & McEvoy, D. J. (2018). Exploring the origins of snow drought in the northern Sierra Nevada, California. *Earth Interactions*, *22*(2), 1–13. https://doi.org/10.1175/ei-d-17-0027.1

Homer, C., Dewitz, J., Yang, L., Jin, S., Danielson, P., Xian, G., et al. (2015). Completion of the 2011 National Land Cover Database for the conterminous United States–representing a decade of land cover change information. *Photogrammetric Engineering & Remote Sensing*, *81*(5), 345–354.

Horton, D. E., Johnson, N. C., Singh, D., Swain, D. L., Rajaratnam, B., & Diffenbaugh, N. S. (2015). Contribution of changes in atmospheric circulation patterns to extreme temperature trends. *Nature*, *522*(7557), 465–469. https://doi.org/10.1038/nature14550

Hunsaker, C. T., Whitaker, T. W., & Bales, R. C. (2012). Snowmelt runoff and water yield along elevation and temperature gradients in California's Southern Sierra Nevada 1. *JAWRA Journal of the American Water Resources Association*, *48*(4), 667–678. https://doi.org/10.1111/j.1752-1688.2012.00641.x

Langenbrunner, B., Neelin, J. D., Lintner, B. R., & Anderson, B. T. (2015). Patterns of precipitation change and climatological uncertainty among CMIP5 models, with a focus on the midlatitude Pacific storm track. *Journal of Climate*, *28*(19), 7857–7872. https://doi.org/10.1175/jcli-d-14-00800.1

Peterson, T. J., Saft, M., Peel, M., & John, A. (2021). Watersheds may not recover from drought. *Science*, *372*(6543), 745–749. https://doi.org/10.1126/science.abd5085

Robeson, S. M. (2015). Revisiting the recent California drought as an extreme value. *Geophysical Research Letters*, *42*(16), 6771–6779. https://doi.org/10.1002/2015gl064593

Rodriguez-Iturbe, I., Porporato, A., Ridolfi, L., Isham, V., & Coxi, D. (1999). Probabilistic modelling of water balance at a point: The role of climate, soil and vegetation. *Proceedings of the Royal Society of London. Series A: Mathematical, Physical and Engineering Sciences*, *455*(1990), 3789–3805. https://doi.org/10.1098/rspa.1999.0477

State of California and the Department of Forestry and Fire Protection. (2021). Fire perimeters through 2020. Retrieved from https://frap.fire.ca.gov/frap-projects/fire-perimeters/

Stephens, S. L., Collins, B. M., Fettig, C. J., Finney, M. A., Hoffman, C. M., Knapp, E. E., et al. (2018). Drought, tree mortality, and wildfire in forests adapted to frequent fire. *BioScience*, *68*(2), 77–88. https://doi.org/10.1093/biosci/bix146

Swain, D. L., Horton, D. E., Singh, D., & Diffenbaugh, N. S. (2016). Trends in atmospheric patterns conducive to seasonal precipitation and temperature extremes in California. *Science Advances*, *2*(4), e1501344. https://doi.org/10.1126/sciadv.1501344

Swain, D. L., Langenbrunner, B., Neelin, J. D., & Hall, A. (2018). Increasing precipitation volatility in twenty-first-century California. *Nature Climate Change*, *8*(5), 427–433. https://doi.org/10.1038/s41558-018-0140-y

Wang, S.-Y. S., Yoon, J.-H., Becker, E., & Gillies, R. (2017). California from drought to deluge. *Nature Climate Change*, *7*(7), 465–468. https://doi.org/10.1038/nclimate3330

Wieczorek, M. (2011). USGS Streamgage NHDPlus version 1 basins 2011.